Damage identification of a flag-shaped hysteresis structure subject to seismic excitation

C. Zhou, J. G. Chase & G. W. Rodgers

Department of Mechanical Engineering, University of Canterbury, Christchurch.

C. Xu

School of Astronautics, Northwestern Polytechnical University, Xi'an, China.

2014 NZSEE Conference

ABSTRACT: This research investigates the structural health monitoring of nonlinear structures after a major seismic event. It considers the identification of flag-shaped or pinched hysteretic behaviour in response to structures as a special, perhaps more general, case of a normal hysteretic curve without pinching.

The method is based on the overall least squares solution and the asymptotic distribution theory of log likelihood ratio. In particular, the structural response is divided into different loading and unloading half-cycles. The overall least squares analysis is first implemented to obtain the minimum residual mean square of each half-cycle regression model with the number of segments assumed. Then the log likelihood ratio test is proposed to assess the likelihood of these nonlinear segments in the presence of noise. The least square fit is finally used for identified segmented regression models to obtain elastic stiffness, plastic stiffness, yielding deformation and energy dissipation parameters. The performance of the proposed method is illustrated using a single degree freedom system and a suite 20 earthquake records. The simulations for this proof of concept include 10% added noise.

The proposed method is computationally efficient and accurate in identifying nonlinear hysteretic structures. These parameters are within 6% average (standard deviation of 10%) of the known values. These results indicate that the system is able to capture highly nonlinear behaviour and structural parameters directly relevant to damage and performance using a computationally efficient and simple method. Finally, the method requires no user input and could thus be automated and performed in real-time for each half cycle.

1 INTRODUCTION

Under conventional seismic design strategy, civil engineering structures are designed to experience inelastic deformation to dissipate earthquake energy, which leads to inevitable residual displacements. Residual deformation increases the repair cost and downtime, as well as the difficulty in recovering the structure system to the initial position. To solve this deficiency, a large number of self-centring systems and devices, which exhibit a flag-shaped hysteretic behaviour, have been developed to avoid residual deformation and provide energy dissipation capacity, such as post-tensioned beam-to-column connections for moment-resisting steel frame (Christopoulos et al. 2002a, Rodgers et al. 2008), steel brace dissipating elements (Bartera et al. 2004, Tremblay et al. 2008) and shape memory alloys (SMA) seismic isolation device (Dolce et al. 2007, Ozbulut et al. 2011). The seismic application of these flag-shaped hysteretic structures has increased since the 1994 Northridge earthquake in the United States and 1995 Hyogoken-Nambu earthquake in Japan. These structures can still experience various degrees or types of damage under extreme excitation. Real-time or rapid structure health monitoring (SHM) can enable the damage state of the structure to be determined, further enabling a more optimum recovery planning after an event.

Many current vibration-based SHM methods are based on the idea that modal parameters change, such as natural frequency, mode shapes and damping, as a result of structural damage (Doebling et al. 1996). However these methods are not robust in the presence of noise and not sensitive to localized damage (Farrar et al. 1994). Further, these method are more applicable to structures where vibration response is highly linear (Chase et al. 2005a).

Damage identification methods based on Eigensystem Realization Algorithm (ERA) are also commonly used for SHM (Lus et al. 2003). The ERA method is based on knowledge of the time domain free response data. These off-line approaches require the entire measured response to process and identify damage and the results might not be immediately available after an event. Adaptive H_∞ filter techniques (Sato et al. 1998) and adaptive fading Kalman filter methods (Loh et al. 2000) can achieve real-time or rapid results. However, they have significant computational cost and complexity. Finally, LMS-based methods have been used for a benchmark problem (Chase et al. 2005a), and also for a highly nonlinear rocking structure (Chase et al. 2005b) to directly identify changes in structural stiffness only. A modified LMS-based method is used to identify both changes in stiffness and plastic deflection (Nayyerloo et al. 2011). However, these LMS approaches are not as effective for nonlinear yielding structures.

This study develops a novel and simplified method to identify the physical parameters that are directly related to structure health monitoring for a flag-shaped hysteretic structure. The performance of proposed method is demonstrated and validated using a simulated flag-shaped hysteretic system. The effect of measurement noise on results is investigated by adding 10% RMS noise to the measured response. The robustness of the results is evaluated using a suite of 20 different earthquake records.

2 METHOD

2.1 Equation of motion

The equation of motion of a single degree of freedom (SDOF) is given by:

$$m\ddot{x} + c\dot{x} + F(x) = -m\ddot{x}_g \tag{1}$$

where x, $\dot{x}$ and $\ddot{x}$ are the displacement, velocity and acceleration of the SDOF system; m is the mass of the system; $F(x)$ is the restoring force of the hysteretic system; and $\ddot{x}_g$ is the ground acceleration; c is the viscous damping coefficient with equation:

$$c = \frac{4m\pi\xi}{T} \tag{2}$$

where ξ is the initial fraction of critical damping; T is the time period of the system.

Using Equation (2), Equation (1) can be rewritten:

$$F(x) = -m(\ddot{x}_g + \ddot{x}) - \frac{4m\pi\xi}{T}\dot{x} \tag{3}$$

In this equation, the acceleration $\ddot{x}$ and $\ddot{x}_g$ can be measured, the velocity and displacement can be obtained from measured acceleration by integration and correction or a range of sensors and methods. Assuming m, ξ and T to be available from the basic knowledge of the system, the value of the restoring force $F(x)$ is consequently obtained. The hysteretic loop of the system can then be constructed.

2.2 Hysteretic Model

Figure 1(a) shows the flag-shaped force-displacement relationship that is representative of a self-centring system hysteretic behaviour. The parameters characterizing the properties of this hysteretic model are α, β and d_y. The coefficient α is the ratio of post-yielding stiffness to pre-yielding stiffness. The energy dissipation coefficient β reflects the dissipation capacity. And d_y is the yield displacement of the hysteretic system. It can be seen that the total restoring force is path dependent. However,

within a time segment where the velocity holds the same sign, the restoring force is a single valued function of displacement. Hence, the whole hysteretic response can be sliced into many sub-half cycles according to the turning points, such as x_4 and x_8, where the velocity is zero.

All the sub-half cycles are then divided into four types of piecewise linear model with one, two, three and four segments respectively, as shown in Figure 1(b). If the numbers of segments of these piecewise linear models could be identified, then the overall least squares solution (Hudson 1966) can be implemented to these linear models and the estimated coefficient of the piecewise linear model will then be related to the system parameters.

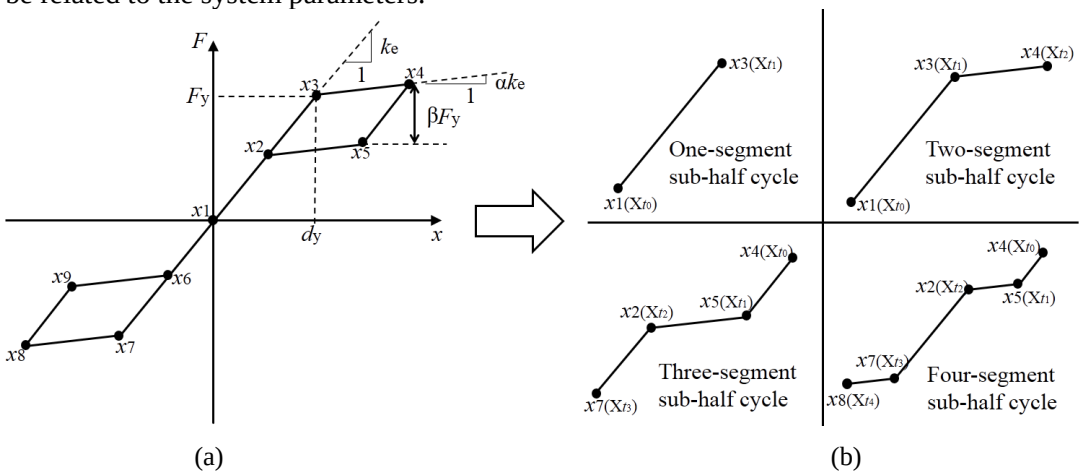

Figure 1. (a) Idealized flag-shaped hysteretic loop, (b) with four types of sub-half cycles

2.3 **Identification procedures**

First, assuming the segments number of the sub-half cycles is r, the r-phase linear model is then defined by (Hudson 1966):

$$\begin{aligned} G(x) = g_1(x) &= a_1 x + b_1 \qquad X_1 = X_{t_0} < x < X_{t_1} \\ &= g_2(x) = a_2 x + b_2 \qquad X_{t_1} < x < X_{t_2} \\ &= g_r(x) = a_r x + b_r \qquad X_{t_{r-1}} < x < X_{t_r} = X_n \end{aligned} \tag{4}$$

where $X_{t_1},\ldots,X_{t_{r-1}}$ are the breakpoints in the sub-half cycles, as shown in Figure 1(b); $(X_1, Y_1),\ldots, (X_n, Y_n)$ are n pairs of displacement and restoring force data during the sub-half cycles, and can be represented by:

$$Y_i = G(X_i) + e_i \qquad i = 1,\ldots,n \tag{5}$$

where e_i is the random errors caused by measurement noise or model uncertainty. Suppose e_i are normally and independently distributed with zero mean and standard deviation σ^2. Then the overall residual sum of squares for r-phase linear model is determined:

$$R_r = \sum_{i=1}^{t_1}[Y_i - g_1(X_i)]^2 + \sum_{i=t_1+1}^{t_2}[Y_i - g_2(X_i)]^2 + \sum_{i=t_{r-1}+1}^{n}[Y_i - g_r(X_i)]^2 \tag{6}$$

The optimum approximate solution to the r-phase linear model is to find the best estimate values of $X_{t_1},\ldots,X_{t_{r-1}}$ to minimise R.

The derivative equal to zero of Equation (3) cannot be used here due to the discontinuous nature of the breakpoints. Thus, the data are divided into every feasible r groups. For each r groups, the standard least linear regression are implemented to obtain the model coefficient $a_1,b_1,\ldots,a_r,b_r$. Then the breakpoints $(X_{t_1},\ldots,X_{t_{r-1}})$ are computed and the residual sum of squares is noted when $X_i \leq X_{t_i} \leq X_{i+1}$. And the solution is the values of $X_{t_1},\ldots,X_{t_{r-1}}$ that correspond to the smallest value of R.

Second, the likelihood-ratio chi square test is used to test the segment number of the sub-half cycles.

The hypothesis test is performed between H_0: there are r segments in this piecewise linear model and H_1: there are r +1 segments in the model. Let λ denote $(R_{r+1}/ R_r)^{n/2}$, then the large sample distribution of the likelihood ratio -2logλ is a chi-squared distribution with 2(r+1) degrees of freedom when the null hypothesis is true (Feder 1975). Therefore, it permits the rejection of H_0 in favour of H_1 when

$$-2\log\lambda \geq \chi^2_\alpha(k) \tag{7}$$

where $P(-2\log\lambda \geq \chi^2_\alpha(k)|H_0)=\alpha$; k is the number of degrees of freedom.

In this study, the significance level α is set to 0.001 and k=2(r+1) for r phase model identification. If the value of likelihood ratio is less than $\chi^2_\alpha(k)$, it suggests that there is no strong evidence against H_0 and it is concluded the sub-half cycle is an r phase model.

The pre-yielding stiffness k_e and post-yielding stiffness k_p can be obtained directly by the regression coefficients of the piecewise linear models identified. And the breakpoints are used to compute the estimates of yield displacement d_y and energy dissipation coefficient β.

The step-by-step procedure is summarized below:

1st step: Assume r=1and r=2 for all the sub-half cycles respectively, and compute R_1, a_1 and b_1 for r=1 and R_2, X_{t_1}, a_1, b_1, a_2 and b_2 for r=2.

2nd step: Compute the likelihood ratio -2logλ for every sub-half cycle and decide the linear sub-half cycles by Equation (7), i.e. $-2\log\lambda<\chi^2_{0.001}(4)$ =18.47.

3rd step: Assume r=3 for all the nonlinear sub-half cycles, and compute R_3, X_{t_1}, X_{t_2}, a_1, b_1, a_2, b_2, a_3 and b_3 for r=3. Then compute -2logλ and get the two segment sub-half cycles by $-2\log\lambda<\chi^2_{0.001}(6)$ =22.46.

4th step: Assume r=4 for the unidentified nonlinear sub-half cycles, and compute R_4, X_{t_1}, X_{t_2}, X_{t_3}, a_1, b_1, a_2, b_2, a_3, b_3, a_4 and b_4 for r=4. Compute -2logλ and identify the three segment sub-half cycles by $-2\log\lambda<\chi^2_{0.001}(8)$ =26.12. The remaining sub-half cycles are then determined as four segment sub-half cycles.

5th step: Estimate physical parameters k_e , k_p ,d_y and β using $X_{t_1},\ldots,X_{t_{r-1}}$ and $a_1,b_1,\ldots,a_r,b_r$.

3 SIMULATED PROOF-OF-CONCEPT STUCTURE

The simulated proof-of-concept structure is a SDOF system that is a representative of a seven storey steel moment resisting frame incorporating post-tensioned energy dissipating connections both at all beam-to-column connections and at the base of each column (Christopoulos et al. 2002b). The structure has a mass of 4000kN and a first period of 1.0s. A 5% constant viscous damping is considered in simulating the structural response. The system behaving flag-shaped hysteretic response has a pre-yielding stiffness of k_e=157.9kN/mm, a post-yielding stiffness of k_p=23.685kN/mm, yield displacement of d_y =24.85mm, and energy dissipation coefficient of β=0.5.

The proposed identification procedure was implemented in Matlab. The simulated structure was subjected to the Loma Prieta earthquake Hollister Differential Array record with peak ground acceleration (PGA) of 0.269g. The system acceleration response was simulated using the Newmark-β integration method. A separate white noise with 10% RMS was added to the simulated acceleration to mimic a more realistic measurement situation. The displacement and velocity were estimated by the low-frequency-measured displacement corrected acceleration integration method (Hann et al. 2009). In this case study, the low-frequency-measured displacement was taken at 1 Hz and acceleration data was taken at 1000Hz.

To assess the robustness of the proposed method over different ground motions, the simulated structure was subjected to a suite of 20 different ground motions (Christopoulos et al. 2002b)The same identified parameters were used for all of the records and 10% RMS noise was added to the simulated acceleration and displacement measurements.

4 RESULTS AND DISCUSSION

Figure 2 shows the identification results for one segment sub-half cycles. The values of -2log λ for one segment sub-half cycles are all less than $\chi^2_{0.001}(4)$ and do not permit the rejection of the one segment model hypothesis by Equation (7). Thus, the sub-half cycles below the rejection value were identified as one segment linear models or simply linear structures.

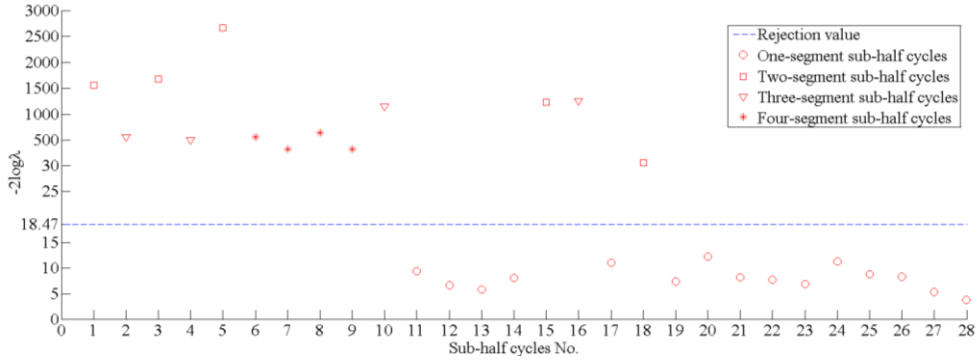

Figure 2. Identification of one segment sub-half cycles

As shown in Figure 3 and Figure 4, the values of -2log λ for two and three segment sub-half cycles are below the rejection value of $\chi^2_{0.001}(6)$ and $\chi^2_{0.001}(8)$, respectively. The sub-half cycles above the rejection value in Figure 4 were identified as four segment linear models with a full flag response.

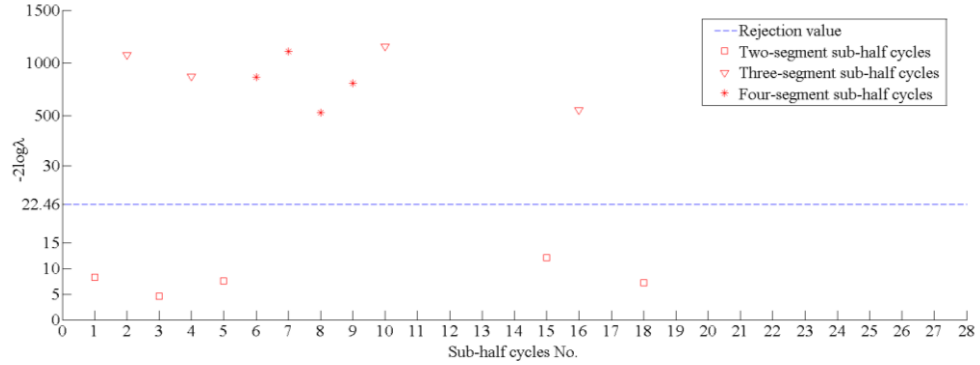

Figure 3. Identification of two segment sub-half cycles, excluding the half cycles found to be one segment

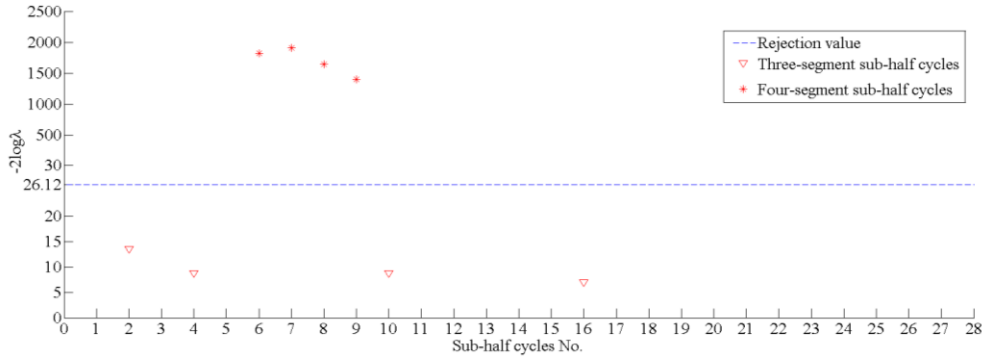

Figure 4. Identification of three and four segment half cycles, excluding one and two segment half cycles

Finally, the segment numbers of all the sub-half cycles were identified and then the physical parameters of structure were obtained in each case using the overall least squares solution. During the earthquake excitation, some sub-half cycles have a very narrow almost negligible plastic part. These small plastic responses have a limited impact on the damage assessment, but affect the accuracy of the parameters estimates. Thus, the displacement increment of the plastic part was used as a threshold to ignore these narrow sub-half cycles for the estimation of the damage parameters. And the effect of ignoring these sub-half cycles on the results was investigated by varying the threshold.

Figure 5 shows the estimates of pre-yielding stiffness and post-yielding stiffness with different threshold. For variable thresholds, the pre-yielding stiffness is robust because the elastic parts for all the sub-half cycles are big enough to obtain good estimates. The post-yielding stiffness is not robust because of the influence of small cycles when the threshold is low.

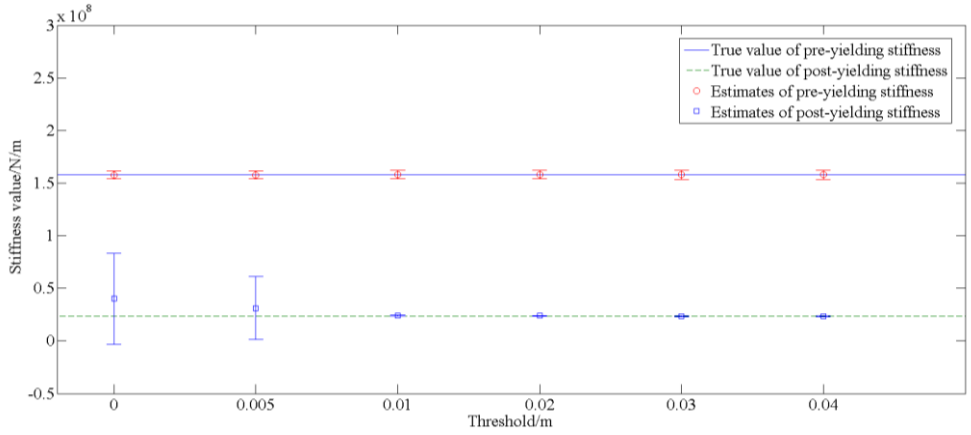

Figure 5. Estimates results of stiffness

Figure 6 and Figure 7 show the estimates of yield displacement and energy dissipation coefficient, respectively. The results are robust with varying thresholds because the turning points used to compute the estimates of d_y and β are not affected by small cycles.

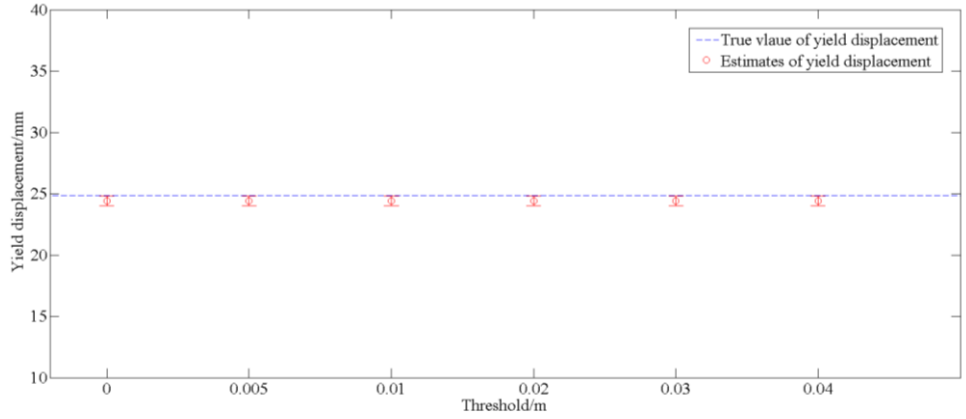

Figure 6. Estimates results of yield displacement

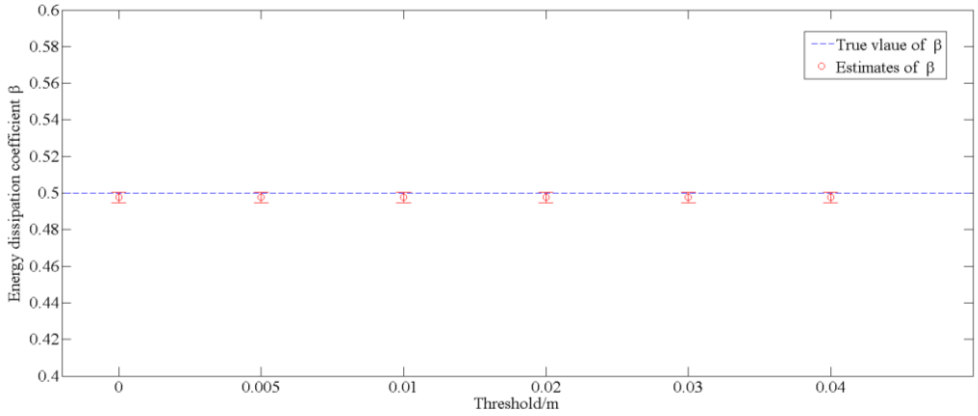

Figure 7. Estimates results of energy dissipation coefficient β

Figure 8 shows the estimates of total absorbed energy. The total energy dissipation dropped as more cycles are ignored with the rising threshold.

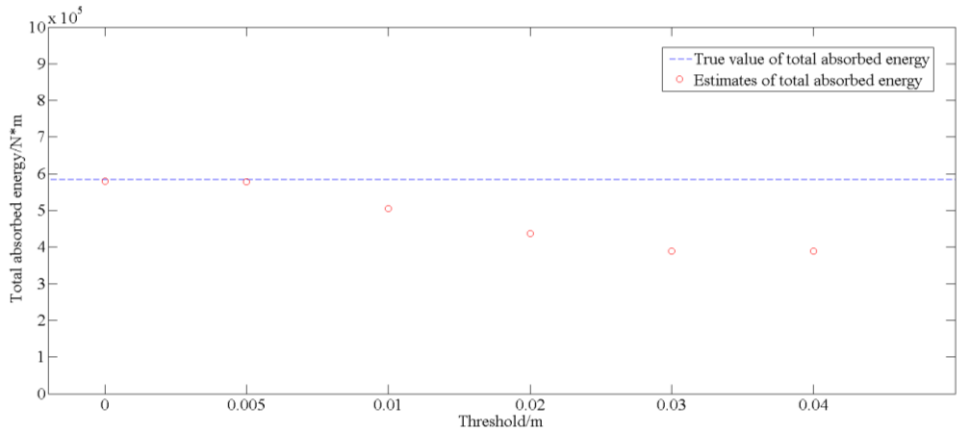

Figure 8. Estimates results of total absorbed energy

As a result, a threshold of 0.04 is chosen to evaluate the results of a 20 suite earthquake records with 10% RMS noise, as shown in Table 1. A '-' is presented where the structure is identified as remaining linear during the entire earthquake.

Table 1. Results for 20 different earthquake events.

Earthquake Record	Pre-yielding stiffness (kN/mm)	Post-yielding stiffness (kN/mm)	Yield displacement (mm)	Energy dissipation coefficient
True	157.9	23.7	24.9	0.500
EQ1	157.4	-	-	-
EQ2	157.0	24.2	25.3	0.508
EQ3	157.7	-	-	-
EQ4	157.1	23.6	25.4	0.503
EQ5	157.8	23.5	23.8	0.495
EQ6	157.8	-	-	-
EQ7	158.7	23.4	24.7	0.496
EQ8	158.8	24.2	24.7	0.500
EQ9	158.6	-	-	-
EQ10	157.7	-	-	-
EQ11	158.2	23.9	24.7	0.478
EQ12	157.9	-	-	-
EQ13	157.5	23.9	24.6	0.498
EQ14	157.9	-	-	-
EQ15	157.8	23.8	24.4	0.498
EQ16	158.1	24.0	24.9	0.479
EQ17	157.7	-	-	-
EQ18	157.2	23.7	24.6	0.492
EQ19	157.6	-	-	-
EQ20	157.9	23.7	23.3	0.527

It can be seen from Table 1 that the mean estimates of k_e, k_p, d_y and β matched well with true input parameters for identified nonlinear events. And the estimates of k_e for identified linear events give a good results as well.

5 CONCLUSIONS

This research develops a simple method for the damage identification of a highly nonlinear flag-shaped hysteretic structure. A simulated system is used to demonstrate the feasibility of the method. The results show that a high threshold can give a good estimates of the physical parameters of the system, and a good estimates of absorbed energy of the system can be obtained with a low threshold. The method is robust to measurement noise even at level of 10%. In addition, good results are obtained for 20 different earthquake events. Overall, the method is computationally simple and can be implemented automatically. Thus, a rapid assessment can be made to offer a significant information of structure damage or safety after an event.

REFERENCES

Bartera, F. & Giacchetti, R. 2004. Steel dissipating braces for upgrading existing building frames. Journal of Constructional Steel Research. 60(3): 751-769.

Chase, J. G., Leo Hwang, K., Barroso, L. & Mander, J. 2005a. A simple LMS‐based approach to the structural health monitoring benchmark problem. Earthquake engineering & structural dynamics. 34(6): 575-594.

Chase, J. G., Spieth, H. A., Blome, C. F. & Mander, J. 2005b. LMS‐based structural health monitoring of a non‐linear rocking structure. Earthquake engineering & structural dynamics. 34(8): 909-930.

Christopoulos, C., Filiatrault, A. & Folz, B. 2002a. Seismic response of self‐centring hysteretic SDOF systems. Earthquake engineering & structural dynamics. 31(5): 1131-1150.

Christopoulos, C., Filiatrault, A., Uang, C.-M. & Folz, B. 2002b. Posttensioned energy dissipating connections for moment-resisting steel frames. Journal of Structural Engineering. 128(9): 1111-1120.

Doebling, S. W., Farrar, C. R., Prime, M. B. & Shevitz, D. W. 1996. Damage identification and health monitoring of structural and mechanical systems from changes in their vibration characteristics: a literature review.

Dolce, M., Cardone, D. & Ponzo, F. C. 2007. Shaking‐table tests on reinforced concrete frames with different isolation systems. Earthquake engineering & structural dynamics. 36(5): 573-596.

Farrar, C. R., Baker, W., Bell, T., Cone, K., Darling, T., Duffey, T., Eklund, A. & Migliori, A. 1994. Dynamic characterization and damage detection in the I-40 bridge over the Rio Grande.

Feder, P. I. 1975. The log likelihood ratio in segmented regression. The Annals of Statistics. 3(1): 84-97.

Hann, C. E., Singh-Levett, I., Deam, B. L., Mander, J. B. & Chase, J. G. 2009. Real-time system identification of a nonlinear four-story steel frame structure—application to structural health monitoring. Sensors Journal, IEEE. 9(11): 1339-1346.

Hudson, D. J. 1966. Fitting segmented curves whose join points have to be estimated. Journal of the American Statistical Association. 61(316): 1097-1129.

Loh, C.-H., Lin, C.-Y. & Huang, C.-C. 2000. Time domain identification of frames under earthquake loadings. Journal of Engineering Mechanics. 126(7): 693-703.

Lus, H., Betti, R., Yu, J. & De Angelis, M. 2003. Investigation of a system identification methodology in the context of the ASCE benchmark problem. Journal of engineering mechanics. 130(1): 71-84.

Nayyerloo, M., Chase, J., MacRae, G. & Chen, X. 2011. LMS-based approach to structural health monitoring of nonlinear hysteretic structures. Structural Health Monitoring. 10(4): 429-444.

Ozbulut, O. E. & Hurlebaus, S. 2011. Seismic assessment of bridge structures isolated by a shape memory alloy/rubber-based isolation system. Smart Materials and Structures. 20(1): 015003.

Rodgers, G. W., Solberg, K. M., Chase, J. G., Mander, J. B., Bradley, B. A., Dhakal, R. P. & Li, L. 2008. Performance of a damage‐protected beam‐column subassembly utilizing external HF2V energy dissipation devices. Earthquake engineering & structural dynamics. 37(13): 1549-1564.

Sato, T. & Qi, K. 1998. Adaptive H∞ filter: its application to structural identification. Journal of Engineering Mechanics. 124(11): 1233-1240.

Tremblay, R., Lacerte, M. & Christopoulos, C. 2008. Seismic response of multistory buildings with self-centering energy dissipative steel braces. Journal of Structural Engineering. 134(1): 108-120.